

WHERE ARE NOBLE GASES TRAPPED IN YAMATO-74063 (UNIQUE)?

Nobuo TAKAOKA¹, Yoshinobu MOTOMURA¹, Kota OZAKI¹
and Keisuke NAGAO²

¹*Department of Earth and Planetary Sciences, Faculty of Science, Kyushu University,
10-1, Hakozaki 6-chome, Fukuoka 812*

²*Institute for Study of the Earth's Interior, Okayama University,
Misasa, Tohaku-gun, Tottori 682-01*

Abstract: Yamato-74063, a primitive achondrite with affinities to Acapulco, has been analyzed for noble gas isotopes by laser ablation mass spectrometry. Some grains released huge amounts of trapped Xe as well as trapped Ar and Kr. Among them, an orthopyroxene grain containing abundant inclusions of tiny metal spherules released equally large amounts of Xe as found for carbon residues of ureilites and carbonaceous chondrites, with $^{36}\text{Ar}/^{132}\text{Xe} = 11$. In contrast, other grains including silicates, Fe-Ni metal and troilite released negligible amounts of trapped gases. Mineralogical studies of polished thin sections, prepared from the same chip as was analyzed for noble gases, indicate that the silicate grains containing the tiny metal inclusions also contain abundant tiny voids, one to several μm across. Originally these voids must have been filled with gases or/and fluids. We propose bubbles as a candidate of hosts that trap large amounts of noble gases in the silicate. With data on noble gas behavior in bubbles, although available only for andesite melt, the extremely low $^{36}\text{Ar}/^{132}\text{Xe}$ ratio in the silicate phase of Y-74063 can be understood in terms of the bubble hypothesis.

1. Introduction

Yamato(Y)-74063, a primitive achondrite with affinities to Acapulco in texture, mineralogy and chemistry, contains large amounts of trapped heavy noble gases (TAKAOKA and YOSHIDA, 1991; TAKAOKA *et al.*, 1993). The Xe concentration for the bulk meteorite is higher than that for most ureilites. The isotopic compositions of Kr and Xe for the bulk, silicate and metal fractions of Y-74063 are homogeneous and identical to those of Q gases (LEWIS *et al.*, 1975; WIELER *et al.*, 1992), indicating that the gases were acquired from a single gas reservoir after most of ^{129}I had decayed to ^{129}Xe . On the other hand, the trapped $^{36}\text{Ar}/^{132}\text{Xe}$ ratio is different among the bulk, silicate and metal, *i.e.*, 22, 17 and 72, respectively. Since the $^{36}\text{Ar}/^{132}\text{Xe}$ ratio for the metal fraction is similar to that for the planetary gas, this indicates that heavy elemental fractionation, *i.e.*, enrichment of Xe relative to Ar, took place at or after noble gas trapping in the silicate, and there are at least two host phases of the trapped gases with high and low Ar/Xe ratios. The trapped gases seem to be concentrated not in specific carrier phases such as carbon and SiC but in major minerals (TAKAOKA *et al.*, 1993). However, the host phases have not been

specified yet. The major aim of this work is to identify the host phase in the Y-74063 primitive achondrite.

2. Experimental

A laser pulse (50 μm in diameter and 1 ms in pulse width) was fired onto a mineral grain and evolved gases were measured by a high sensitivity noble gas mass spectrometer. In order to extract gases from a single grain without penetrating it into underlying grains, a low energy (25 mJ) pulse was employed except for pit 22 for which a 50 mJ pulse was used. In all other respects, the analytical techniques are the same as those employed by TAKAOKA *et al.* (1993). Further information is found in NAGAO and ABE (1994) on the laser probe mass spectrometry of meteoritic noble gases.

The weight of melt produced by a laser shot was estimated by dividing cosmogenic ^3He released by the concentration of cosmogenic ^3He determined for the silicate and metal fractions (TAKAOKA *et al.*, 1993), assuming 100% extraction yield for cosmogenic ^3He . The concentration of cosmogenic ^3He for troilite was calculated using the data for both fractions and the relative production rates from metal and other elements (BOGARD and CRESSY, 1973). As shown in Table 1, the weight of melt for pit 23 to 37 was estimated to be 0.4, 0.8 and 0.9 μg , on average, for silicates, troilite and Fe-Ni metal, respectively. From these values and the density of the respective mineral, the depth of a pit was calculated to be 31 μm for silicates, 29 μm for metal, and 55 μm for troilite, assuming a constant diameter of 67 μm that is the average of pit diameters measured on the repolished section. For pit 22, the melt weight and the depth of pit are 1.5 μg and 120 μm , respectively. Because the silicate grain probed by pit 22 is about 160 μm across (a geometrical mean for long and short diameters), as shown in Fig. 1, pit 22 may have penetrated the grain into underlying material. The size of the investigated silicate grains is almost 160 μm across, while the size of metal and troilite grains is about 80 μm . The orthopyroxene grain for pit 27 is some 180 μm across, and therefore, the probability that pit 27 penetrated the grain into underlying material is small.

The released gases were measured with a noble gas mass spectrometer (Modified VG5400) using ion counting techniques at Okayama University. Noble gas blanks are: $^4\text{He} = 2 \times 10^{-12}$, $^{36}\text{Ar} = 6 \times 10^{-13}$, $^{84}\text{Kr} = 8 \times 10^{-15}$ and $^{132}\text{Xe} = 1 \times 10^{-15}$ cm^3STP . Because of extremely small sample size, no data are available for Ne. The abundance for noble gas X from pit j is represented by the normalized release $NR(X)$ (TAKAOKA *et al.*, 1993),

$$NR(X)_j = C(^3\text{He})[X]_j / [^3\text{He}]_j,$$

where $C(^3\text{He})$, $[X]_j$ and $[^3\text{He}]_j$ are the concentrations of cosmogenic ^3He , amounts of gas X and cosmogenic ^3He released from pit j , respectively. Efficiency of extraction recovery is assumed to be 100%, *i.e.*, all ^3He in the melt was released. Generally the extraction efficiency of trapped gases is higher for lighter gases relative to heavier ones. Therefore, the elemental ratio such as $^{36}\text{Ar}/^{132}\text{Xe}$ should be

regarded as an upper limit of the ratio.

The sample analyzed in this work is the same as that analyzed by TAKAOKA *et al.* (1993). It was repolished to remove the melt splash that adhered to the sample from the previous study. We tried to inspect the polished sample using a microscope with reflected light, but unfortunately, the sample adhered on a metal base and detailed inspection with transmitted light was impossible. For further mineralogical study, we used other polished thin sections (PTS) of 150 μm thickness that were prepared from the same chip as that analyzed in the laser experiment. They were inspected with the optical microscope with transmitted and reflected light and with an electron probe microanalyzer (JXA-733).

3. Results and Discussion

3.1. Noble gas analyses

The results of the noble gas analyses are given in Table 1, together with data for the bulk meteorite for comparison. The most prominent result is the release of huge amounts of Xe as well as Ar and Kr from pit 27 in orthopyroxene containing tiny metal inclusions. The normalized release of ^{132}Xe is extremely high, $8.5 \times 10^{-7} \text{ cm}^3\text{STP/g}$ with $^{36}\text{Ar}/^{132}\text{Xe} = 11$. This cannot be attributed to the difference in the extraction yield between cosmogenic He and trapped Xe, because the preferential release of ^3He would result in an even higher Xe concentration. The amount of radiogenic ^{40}Ar released from pit 27 is lower than the blank level. This is consistent with a general tendency of low K in orthopyroxene.

Pits 22, 26 and 36 in silicate, FeS, and silicate with tiny metal inclusions, respectively, also released large amounts of Xe and Ar except for pit 26 which yielded a low Ar abundance. The high abundance of radiogenic ^{40}Ar for pits 22 and 36 indicates that these pits may have penetrated K-rich minerals such as plagioclase. As mentioned earlier, it is very likely that the depth of pit 22 extends to underlying grains. The high abundance of trapped gas may either be released from underlying grains, or the grain for pit 22 may be rich in the tiny metal inclusions inside it. In contrast, some grains such as pits 24, 25, 29 and 30 give low releases of trapped gases. They are silicate, Fe-Ni metal, and FeS grains. The silicate grain (pit 24) is clear and free from inclusions, when observed with reflected light.

Enrichment of trapped gases in silicates with tiny metal inclusions agrees with our previous result (TAKAOKA *et al.*, 1993), confirming that the silicate grains containing tiny metal inclusions contain large amounts of trapped gases and that silicate grains without such inclusions show low abundances of trapped gases. The present result also indicates that some grains of FeS give large releases of trapped gases. However, as mentioned above, the pit depth (55 μm) estimated for FeS is rather deep compared to its grain size, therefore, we cannot rule out possible degassing from underlying grains.

3.2. Mineralogical study

Figure 1 displays photomicrographs of the polished sample, including pits 22,

Table 1. Normalized releases and isotopic ratios of noble gases determined for Y-74063 primitive achondrite by laser ablation mass spectrometry. Data for bulk of Y-74063 are also given for comparison.

Pit No.	Weight of melt (μg)	$^4\text{He}^{1)}$	$^{36}\text{Ar}^{1)}$	$^{84}\text{Kr}^{2)}$	$^{132}\text{Xe}^{2)}$	$^3\text{He}/^4\text{He}$	$^{38}\text{Ar}/^{36}\text{Ar}$	$^{40}\text{Ar}/^{36}\text{Ar}$	Remarks
22	1.46	56.7 ± 5.8	4.1 ± 0.5	44 ± 25	138 ± 15	0.0022 ± 0.0003	0.194 ± 0.005	8.8 ± 5.6	silicate
23	0.25	9.8 ± 2.7	2.1 ± 0.6	10 ± 76	16 ± 6	0.0126 ± 0.0054	0.199 ± 0.049	52 ± 58	silicate (inclusion)
24	0.54	5.9 ± 1.5	0.1 ± 0.2	n.d. ³⁾	4 ± 5	0.0214 ± 0.0030	0.31 ± 0.63	n.d. ³⁾	silicate
25	0.95	2.8 ± 0.6	n.d. ³⁾	14 ± 24	4 ± 5	0.0257 ± 0.0035	n.d. ³⁾	n.d.	Fe-Ni
26	1.3	12.7 ± 1.5	0.3 ± 0.1	5 ± 6	166 ± 18	0.0073 ± 0.0006	0.221 ± 0.051	20 ± 73	FeS
27	0.52	6.1 ± 1.4	9.0 ± 1.0	87 ± 23	850 ± 91	0.0207 ± 0.0027	0.191 ± 0.005	n.d.	silicate (inclusion)
28	0.67	5.8 ± 1.3	1.0 ± 0.2	17 ± 18	21 ± 4	0.0164 ± 0.0027	0.213 ± 0.032	142 ± 31	FeS
29	0.79	4.8 ± 0.9	0.2 ± 0.1	7 ± 21	4 ± 2	0.0198 ± 0.0024	0.33 ± 0.12	260 ± 120	FeS
30	0.34	10.0 ± 2.3	1.0 ± 0.3	n.d.	4 ± 2	0.0125 ± 0.0034	0.185 ± 0.050	35 ± 74	silicate
31	0.78	3.4 ± 1.0	0.1 ± 0.1	1 ± 14	62 ± 9	0.0212 ± 0.0057	0.23 ± 0.13	92 ± 203	Fe-Ni
32	0.36	40.0 ± 4.8	13.5 ± 1.6	26 ± 37	71 ± 11	0.0031 ± 0.0008	0.191 ± 0.008	15.0 ± 5.4	silicate
33	0.36	18.8 ± 3.1	0.2 ± 0.2	n.d.	49 ± 7	0.0067 ± 0.0016	n.d.	1070 ± 870	silicate
34	0.37	10.4 ± 2.5	2.2 ± 0.4	9 ± 27	15 ± 3	0.0119 ± 0.0038	0.192 ± 0.025	109 ± 27	silicate
35	0.33	15.1 ± 2.9	1.3 ± 0.3	6 ± 36	11 ± 7	0.0086 ± 0.0014	0.187 ± 0.034	117 ± 45	silicate
36	0.49	16.5 ± 2.3	15.9 ± 1.7	35 ± 42	96 ± 13	0.0103 ± 0.0013	0.193 ± 0.006	4.8 ± 3.1	silicate (inclusion)
37	0.54	5.4 ± 1.1	0.0 ± 0.1	6 ± 23	15 ± 3	0.0182 ± 0.0026	n.d.	n.d.	FeS
Bulk		27.0	1.5	55.3	66.5	0.00475 ± 0.00030	0.1898 ± 0.0009	33.91 ± 0.10	TAKAOKA <i>et al.</i> (1993)

¹⁾ Abundances of He and Ar are given in units of $10^{-6} \text{cm}^3 \text{STP/g}$. Errors cited include counting statistics, and uncertainties for blank correction and the abundances of standard gases, but do not include those for weight of melt.

²⁾ Abundances of Kr and Xe are given in units of $10^{-9} \text{cm}^3 \text{STP/g}$. Errors cited include counting statistics, and uncertainties for blank correction and the abundances of standard gases, but do not include those for weight of melt.

³⁾ n.d.: Not determined because measured amounts were lower than blank.

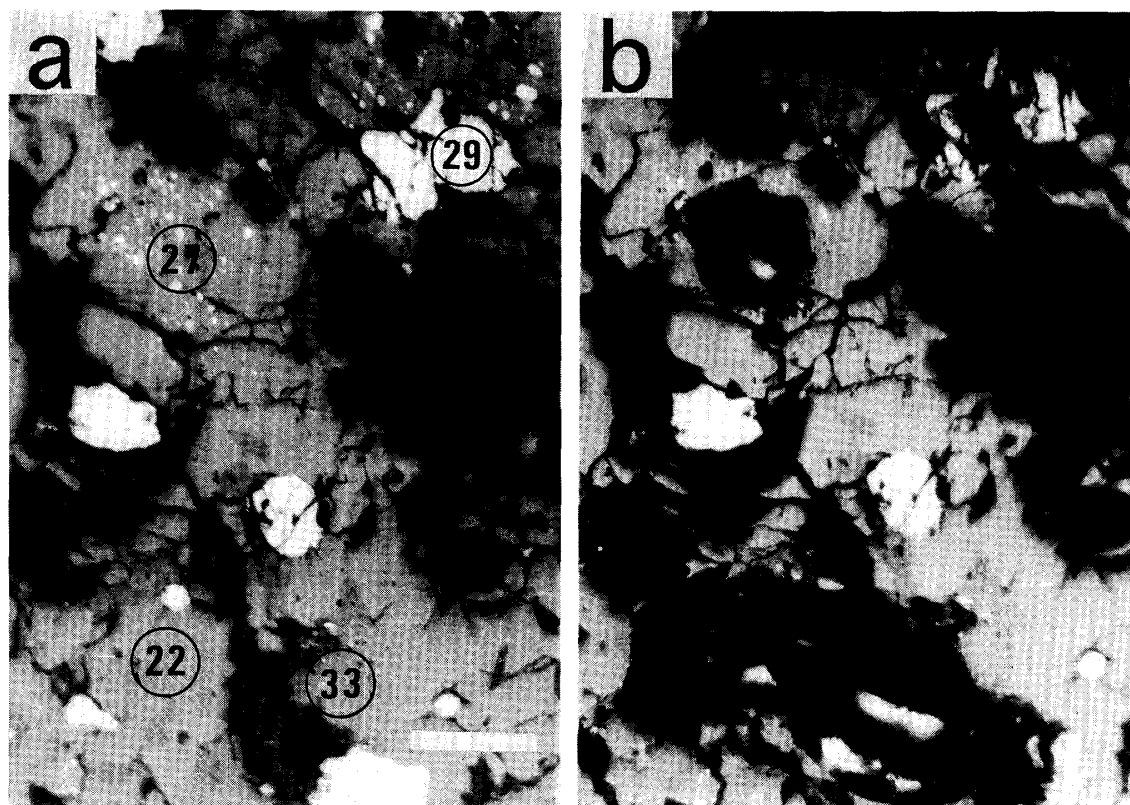
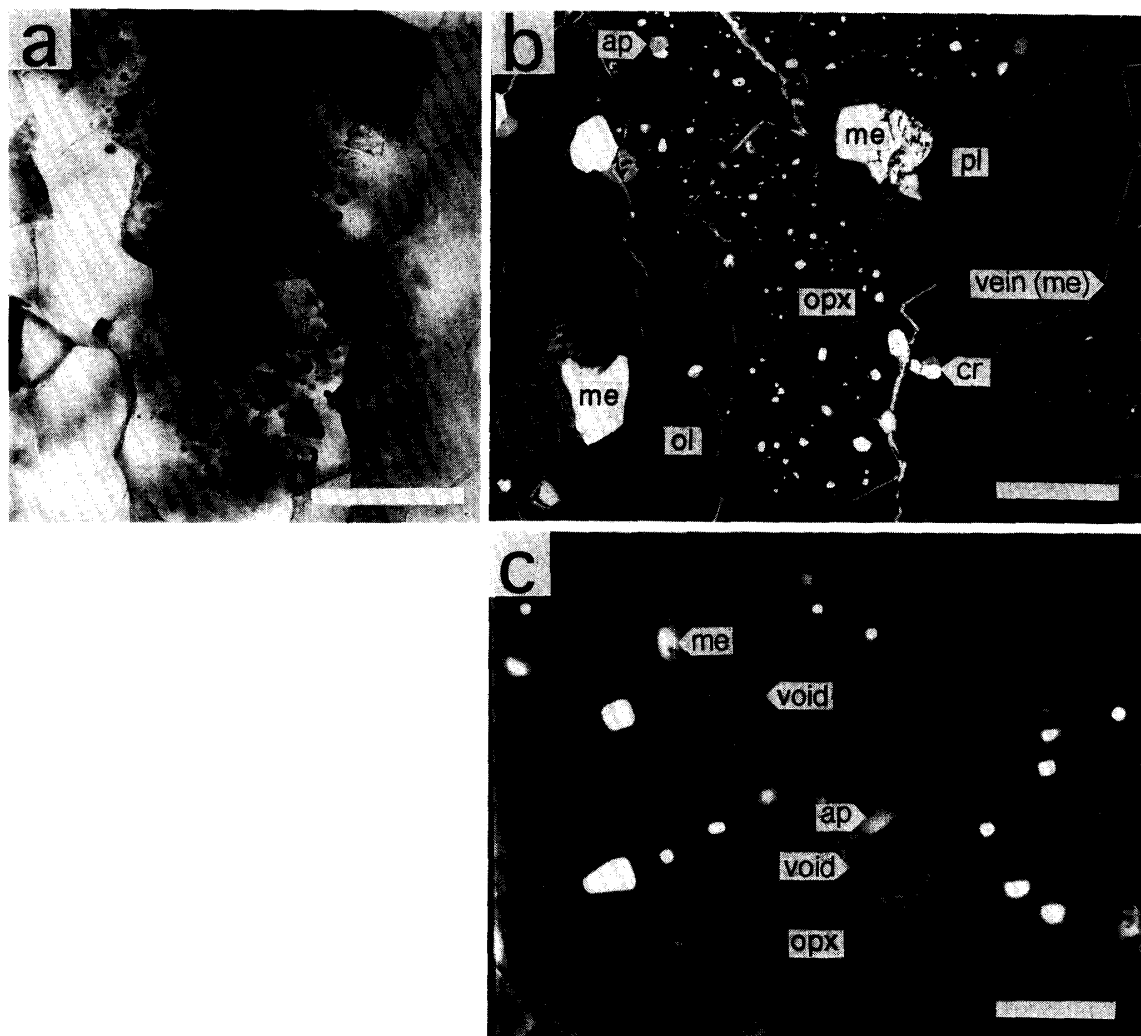


Fig. 1. Photomicrographs of the sample including pits 22, 27, 29 and 33, taken before (a) and after (b) laser shots with reflected light. White inclusions in orthopyroxene for pit 27 are metal. The large black area on the right is a pit site from a previous study. The others are due to breakage during polishing. White scale bar: 100 μm .

27, 29 and 33, taken before and after laser shots with reflected light. The grain for pit 27 contains plenty of tiny, white and black inclusions. Since this sample was unsuitable for the mineralogical study with transmitted light, we inspected the other PTS's prepared from the same chip as used in the laser experiment, as mentioned above.

Figure 2 displays a photomicrograph of grains containing the tiny metal inclusions with transmitted light and back-scattered electron images of the same area. From the back-scattered electron images and semi-quantitative analyses, white inclusions in Fig. 2b are mostly metallic. Black ones in Fig. 2b and 2c are mostly voids that could be distinguished from black plugs with reflected light. The voids range in size from one to several μm across. They are not artifacts due to the preparation of the PTS, but indigenous, because inclusions with opaque minerals on walls are found on both the surface (Fig. 2c) and the inside of PTS's with transmitted light. Originally such voids must have been filled with gases or/and fluids. With transmitted light, many small inclusions are visible that are round to oval in shape and similar to bubbles or fluid inclusions. A cooling-heating experiment is planned to study the solidification and homogenization temperatures of such inclusions.

A notable feature found in Fig. 2 is that the tiny metal inclusions accompanied



Figs. 2a, b. Photomicrograph with transmitted light (Fig. 2a) and back-scattered electron images (Fig. 2b) of grains (orthopyroxene: *opx*) containing many tiny metal inclusions. The sample is PTS prepared from the same chip as used in the laser experiment. In Fig. 2b, white inclusions and veins are composed mostly of metal (*me*). Apatite (*ap*) and chromite (*cr*) are also found. Large black grains are plagioclase (*pl*). White scale bar: 50 μm .

Fig. 2c. Back-scattered electron images enlarging the uppermost grain in Fig. 2b. Three voids with metal (*me*) and apatite (*ap*) on the walls are found in orthopyroxene crystals. Whitish rings around voids are not due to enrichment of heavy elements but halos are due to enhanced electron scattering on edge. With transmitted light, clear *opx* and olivine (*ol*) crystals free from inclusions are adjacent to *opx* crystals with dusty inclusions. Black dots are mostly voids that can be distinguished from black plugs, if any, with reflected light. White scale bar: 10 μm .

by bubbles do not occur ubiquitously in all grains. The orthopyroxene grains containing the tiny inclusions are adjacent to olivine and pyroxene that are free from such inclusions. The Fe concentration is very similar in orthopyroxene grains with and without tiny metal inclusions (FeO: 7.0 and 6.9 wt%, respectively), indicating that they are not in-situ products by the reduction of host orthopyroxene. In addition, tiny transparent inclusions of various shapes and sizes are found with

transmitted light. Inclusions observed on the surface of PTS are simple in shape. Probably we observe the cross sections of inclusions of irregular shape in three dimensions. They are composed of olivine. No glass inclusions are found on the PTS surface.

There are two distribution patterns of inclusions. One reveals a broad distribution in three dimensions, as found in Fig. 2. Pit 27 was shot to a grain showing such a distribution. The other one shows a linear distribution (Fig. 3). In addition, the former appears to be richer in metal than the latter. Depth profiles given in Fig. 3b to 3f are sketches drawn out by changing the focussing depth of a microscope. At a

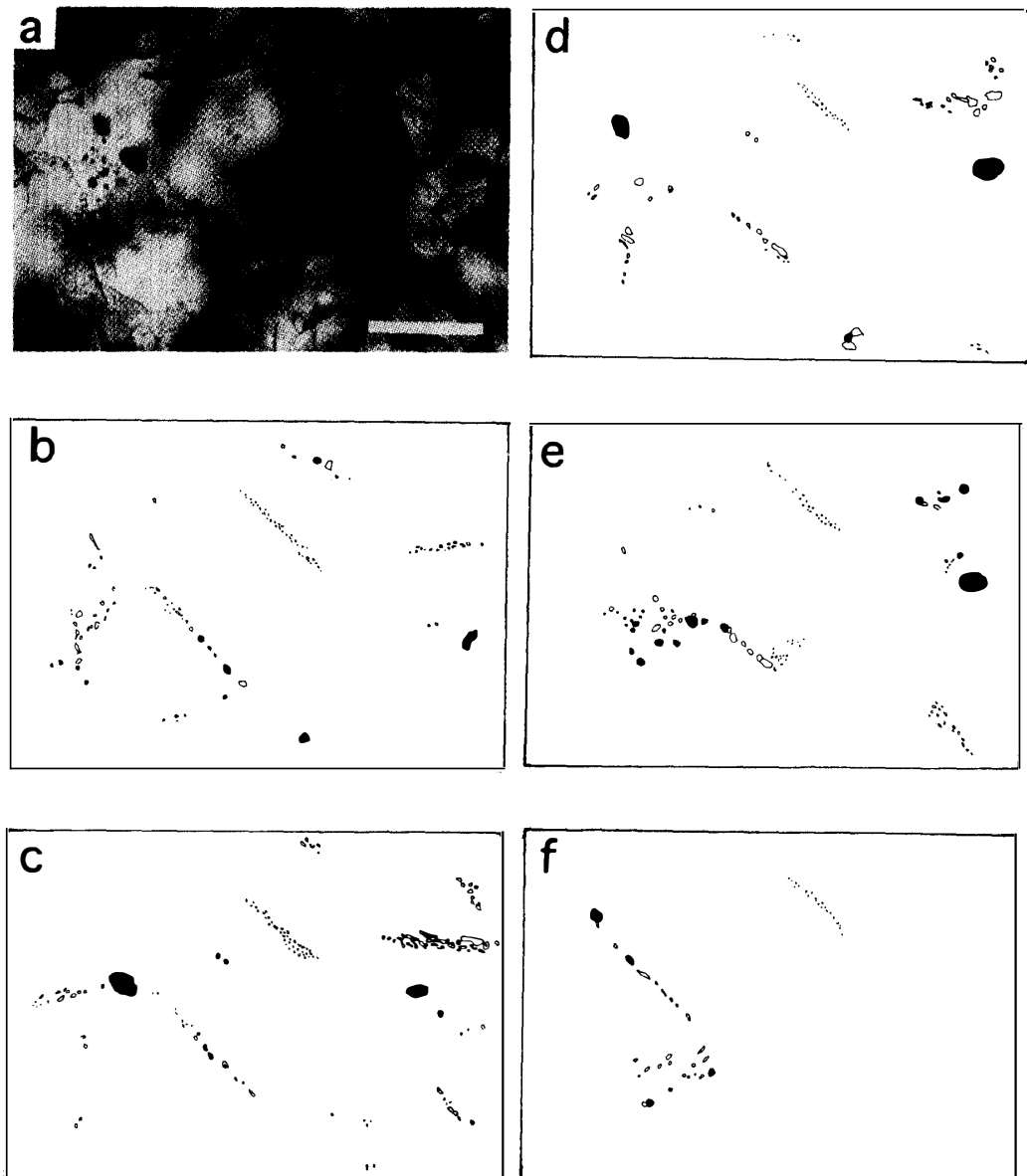


Fig. 3a. Photomicrograph of grain containing linear trains of inclusions with transmitted light. White scale bar: 50 μm .

Figs. 3b-3f. Depth profiles drawn out by changing the focusing depth of a microscope. Oriented sets of linear trains suggest the existence of extinct fractures in crystals. Opaque inclusions are black; others are transparent.

constant depth, we can find oriented sets of linear trains of inclusions, and in three dimensions they appear to be distributed along curved fractures, although some variations are found. This is very suggestive of the properties and the origin of the inclusions, as will be discussed later.

3.3. Bubbles as a host for trapped gases: A speculation

The abundance of ^{132}Xe released from pit 27 is comparable with that for carbon residues of ureilites (GÖBEL *et al.*, 1978) and carbonaceous chondrites (WIELER *et al.*, 1992), as shown in Fig. 4. This requires that all the material molten by a laser shot is carbon, if carbon is the host phase of the trapped gas. This is not the case because the melt consists mostly of silicate and metal. Although NAGAHARA *et al.* (1990) have reported graphite as accessory mineral, we find no graphite in our sample. This is consistent with the origin of the meteorite by partial melting in a melt pocket of the parent body (NAGAHARA *et al.*, 1990). If carbon was present before partial melting, most of it should have been exhausted to reduce silicates at the high temperature to which the stone material was partially molten. So we propose bubbles as a host for the trapped noble gases which show extremely high noble gas abundance and very low Ar/Xe ratio. The possibility that microbubbles in ortho-

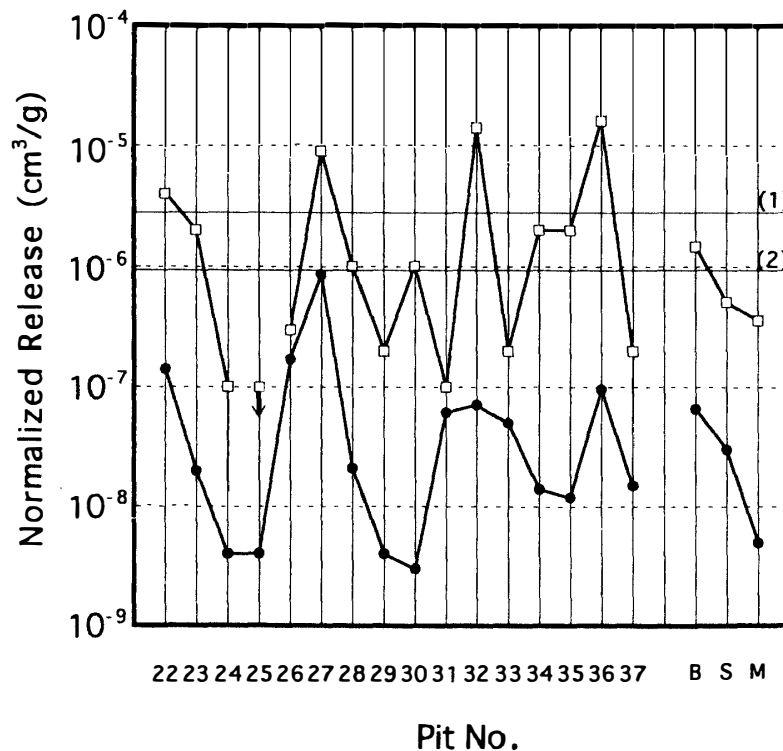


Fig. 4. ^{36}Ar (\square) and ^{132}Xe (\bullet) abundances released by a laser shot. The abundances for bulk (B), silicate (S) and metal (M) are also presented for comparison (TAKAOKA *et al.*, 1993). Some grains released large amounts of trapped gases. The ^{132}Xe abundance for pit 27 is comparable with that for carbon residues of ureilites and carbonaceous chondrites. Horizontal lines (1) and (2) represent the ^{132}Xe abundances for carbon residues of Dyarpur ureilite (GÖBEL *et al.*, 1978) and Murchison carbonaceous chondrite (WIELER *et al.*, 1992), respectively.

pyroxene in Acapulco might contain large amounts of noble gases has been put forward by KIM and MARTI (1993).

As indicated by the low Fa and Fs contents in olivine and pyroxene, respectively, the meteorite has experienced a reducing environment (YANAI and KOJIMA, 1991), although the reducing agent is unknown. One plausible candidate is carbon. Carbon in chondrites is usually concentrated in the matrix (VAN DER STAP *et al.*, 1986) and carbon coating of the surface of troilite and metal grains has been reported by MAKJANIC *et al.* (1993). Ureilites contain carbon veins, and noble gases in ureilites are trapped in diamond (GÖBEL *et al.*, 1978) and amorphous carbon (WACKER, 1986). Trapped gases in carbonaceous chondrites also reside in carbon. So-called Q-gases that contribute more than 90% of primordial Ar, Kr and Xe were released by oxidation of acid resistant residues of carbon (WIELER *et al.*, 1992).

When carbon is heated together with silicates, it should serve as a reducing agent and be oxidized itself to CO or finally CO₂. Gases trapped in carbon would be released to the ambient gas phase or the melt together with CO or CO₂ that could serve as a carrier agent. The ambient atmosphere including noble gases could be trapped along a fracture of a preexisting crystal and enclosed therein as a result of rehealing of the fracture. The gases dissolved into the melt would diffuse to grain boundaries. The gas atoms would concentrate at grain boundaries to swell up to bubbles. Such examples of He bubbles (3 to 30 nm across) that swelled along grain boundaries have been clearly observed in SiC (SASAKI *et al.*, 1991). Once bubbles originated in mineral grains, noble gases could concentrate therein because they are distributed preferentially in the gas phase.

Figure 3 shows oriented linear trains of inclusions inside a crystal, indicating the existence of extinct fractures. The linear pattern suggests the secondary origin of inclusions, *i.e.*, the inclusions formed after the crystallization of the host mineral. However, the broad distribution (Fig. 2) is difficult to understand assuming a secondary origin. As mentioned above, the metal spherules are not *in-situ* products from the reduction of silicates. It is very likely that the metal spherules were carried by the melt from the production scene and embedded in a new crystal which grew in the carrier agent. Bubbles that followed them could have been trapped in the same crystal. Because of the old Ar-Ar age (4556 ± 56 Ma; KANEOKA *et al.*, 1992), we suggest that the enclosure of inclusions took place during the crystallization in the melt pocket of the parent body. A process related to melt migration might have played an important role in enriching this stone in noble gases and tiny metal spherules.

To confirm the bubble hypothesis, the next step would be to determine the major component of the bubble gases which are released with the trapped noble gases. It is certain that considerable amounts of gases, although the composition is unknown, were released. When a laser pulse was fired, the pressure in the purification line increased to 10^{-7} Torr and decreased to 10^{-9} Torr after a few seconds. The quick change in pressure indicates that the evolved gases are not adhesive and are removed easily by getter.

An additional goal is to understand which mechanisms caused enrichment and

fractionation of the noble gases. In terms of the bubble hypothesis, the abundance of bubble gas is estimated to be 10^{-7} cm³STP, if we assume a pressure of 10^{-7} Torr in the purification line with a volume of about 10^3 cm³. Assuming all bubble gas to be CO or CO₂, the atomic ratio of trapped ¹³²Xe to C (5×10^{-6}) is four orders of magnitude larger than that for the carbon residues (5×10^{-10}), requiring enrichment of Xe by a factor of 10^4 .

The difference in the ³⁶Ar/¹³²Xe ratio between the metal and silicate fractions (TAKAOKA *et al.*, 1993) requires a fractionation mechanism. A plausible mechanism involving bubbles has been reported by LUX (1987). Enrichment of noble gases compared to the starting composition has been found for bubbles in andesite melt. LUX attributed this to shrinkage of bubbles by quenching after a net inward migration of noble gases at high temperature. It is accompanied by preferential solution and diffusion of light gases into silicates, resulting in the enrichment of heavy gases relative to light ones in bubbles. She observed an enrichment of Xe by a factor of 5 relative to Ar for bubbles in andesite melt. However, data on enrichment and fractionation of noble gases, for which bubbles are responsible, are available only for the andesite melt. We need more data to understand the role of bubbles in noble gas cosmochemistry because occlusion of bubbles is an important mechanism for trapping gases in minerals. It is inferred that this mechanism works effectively in rocks that experienced partial melting, because at higher temperature, the formation of a long-range network of bubbles would open a route along grain boundaries to the free surface (SASAKI *et al.*, 1991) and enlarged bubbles could migrate upward by buoyancy.

4. Conclusions

(1) Some grains released huge amounts of trapped Ar, Kr and Xe. Among them, the abundance of Xe for an orthopyroxene grain is comparable with that for carbon residues of ureilites and carbonaceous chondrites. This grain contains abundant inclusions of tiny bubbles as well as tiny metal spherules. There is a tendency for silicate grains containing the tiny metal inclusions to be rich in both trapped gases and bubbles.

(2) We propose bubbles as a candidate for the host site of trapped noble gases in the silicate phase of Y-74063. The extremely low ³⁶Ar/¹³²Xe ratio observed in the silicate can be understood in terms of the bubble hypothesis.

(3) Measurements of the major trapped component and determinations of solidification and homogenization temperatures by a cooling-heating experiment for grains containing gas or/and fluid-filled bubbles might confirm the bubble hypothesis. Further, we suggest study of the noble gas enrichment and fractionation in bubbles for a variety of silicate melts.

(4) In spite of these problems, the present result indicates that not only adsorption and solution but also occlusion of bubbles can play an important role in noble gas cosmochemistry, in particular for rocks heated to partial melting.

Acknowledgments

This work forms part of the consortium study of unique meteorites. The authors thank Drs. I. KUSHIRO and H. NAGAHARA for organization of the consortium study. They are also grateful to Drs. K. YANAI and H. KOJIMA for the sample. The authors wish to extend their thanks to Drs. O. EUGSTER and J.-I. MATSUDA for their reviews and constructive comments.

References

- BOGARD, D. D. and CRESSY, P. J. (1973): Spallation production of ^3He , ^{21}Ne , and ^{38}Ar from target elements in the Bruderheim chondrite. *Geochim. Cosmochim. Acta*, **37**, 527–546.
- GÖBEL, R., OTT, U. and BEGEMANN, F. (1978): On trapped gases in ureilites. *J. Geophys. Res.*, **83**, 855–867.
- KANEOKA, I., TAKAOKA, N. and YANAI, K. (1992): ^{40}Ar - ^{39}Ar analyses of Y-74063 and ALH-78230: Consortium study on unique meteorites from Antarctica. *Proc. NIPR Symp. Antarct. Meteorites*, **5**, 224–232.
- KIM, Y. and MARTI, K. (1993): Isotopic signatures and distribution of nitrogen and trapped and radiogenic xenon in the Acapulco and FRO-90011 meteorites. *Lunar and Planetary Science XXIV*. Houston, Lunar Planet Inst., 801–802.
- LEWIS, R. S., SRINIVASAN, B. and ANDERS, E. (1975): Host phase of a strange xenon component in Allende. *Science*, **190**, 1251–1262.
- LUX, G. (1987): The behavior of noble gases in silicate liquids: Solution, diffusion, bubbles and surface effects, with applications to natural samples. *Geochim. Cosmochim. Acta*, **51**, 1549–1560.
- MAKJANIC, J., VIS, R. D., HOVENIER, J. W. and HEYMANN, D. (1993): Carbon in the matrices of ordinary chondrites. *Meteoritics*, **28**, 63–70.
- NAGAHARA, H., FUKUOKA, T., KANEOKA, I., KIMURA, H., KUSHIRO, I., TAKEDA, H., TSUCHIYAMA, A. and YANAI, K. (1990): Petrology of unique meteorites, Y-74063, Y-74357, Y-75261, Y-75274, Y-75300, Y-75305, A-77081, A-78230, and A-8002. Papers Presented to the 15th Symposium on Antarctic Meteorites, May 30–June 1, 1990. Tokyo, Natl Inst. Polar Res., 92–94.
- NAGAO, K. and ABE, T. (1994): Application of laser to spot analysis of noble gases in primitive meteorite. *J. Mass Spectrom. Soc. Jpn.*, **42**, 35–48.
- SASAKI, K., YANO, T., MURAYAMA, T. and ISEKI, T. (1991): Helium release and micro structure of neutron-irradiated SiC ceramics. *J. Nucl. Mater.*, **179–181**, 407–410.
- TAKAOKA, N. and YOSHIDA, Y. (1991): Noble gas composition in unique meteorite Yamato-74063. *Proc. NIPR Symp. Antarct. Meteorites*, **4**, 178–186.
- TAKAOKA, N., NAGAO, K. and MIURA, Y. (1993): Noble gases in the unique meteorites Yamato-74063 and -74357. *Proc. NIPR Symp. Antarct. Meteorites*, **6**, 120–134.
- VAN der STAP, C. C. A. H., HEYMANN, D., VIS, R. D. and VERHEUL, H. (1986): Mapping of carbon concentrations in the Allende meteorite with the $^{12}\text{C}(\text{d}, \text{p})^{13}\text{C}$ method. *Proc. Lunar and Planet. Sci. Conf.*, 16th, Part 2, D373–D377 (*J. Geophys. Res.*, **91**, B4).
- WACKER, J. F. (1986): Noble gases in the diamond-free ureilite, ALHA78019: The roles of shock and nebular processes. *Geochim. Cosmochim. Acta*, **50**, 633–642.
- WIELER, R., ANDERS, E., BAUR, H., LEWIS, R. S. and SIGNER, P. (1992): Characterization of Q-gases and other noble gas components in the Murchison meteorite. *Geochim. Cosmochim. Acta*, **56**, 2907–2921.
- YANAI, K. and KOJIMA, H. (1991): Yamato-74063: Chondritic meteorite classified between E and H chondrite groups. *Proc. NIPR Symp. Antarct. Meteorites*, **4**, 118–130.

(Received July 29, 1993; Revised manuscript received September 28, 1993)